



Revisiting the Cygnus OB associations

Author: Alexis L. Quintana and Nicholas J. Wright

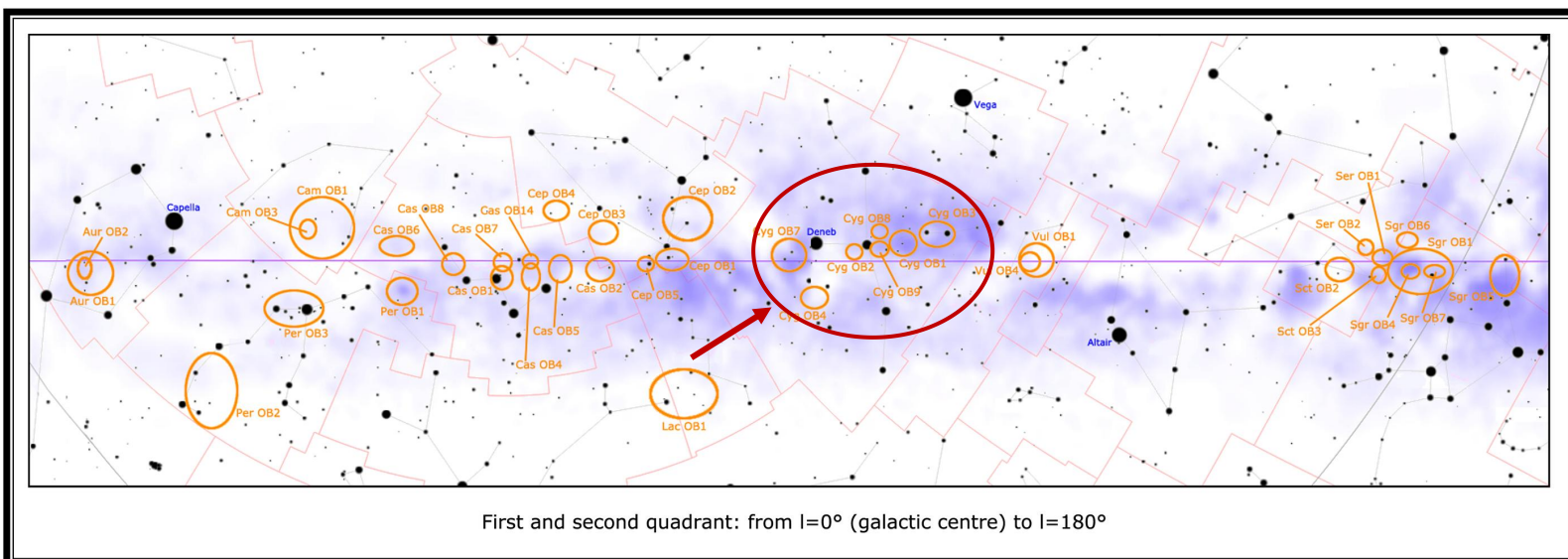
Reporter: Yanan Cao

Outline

- Introduction
- The Existing OB Associations In Cygnus
- Identifying And Characterizing OB Stars
- Analysis of the New OB Associations
- Discussion and Conclusion

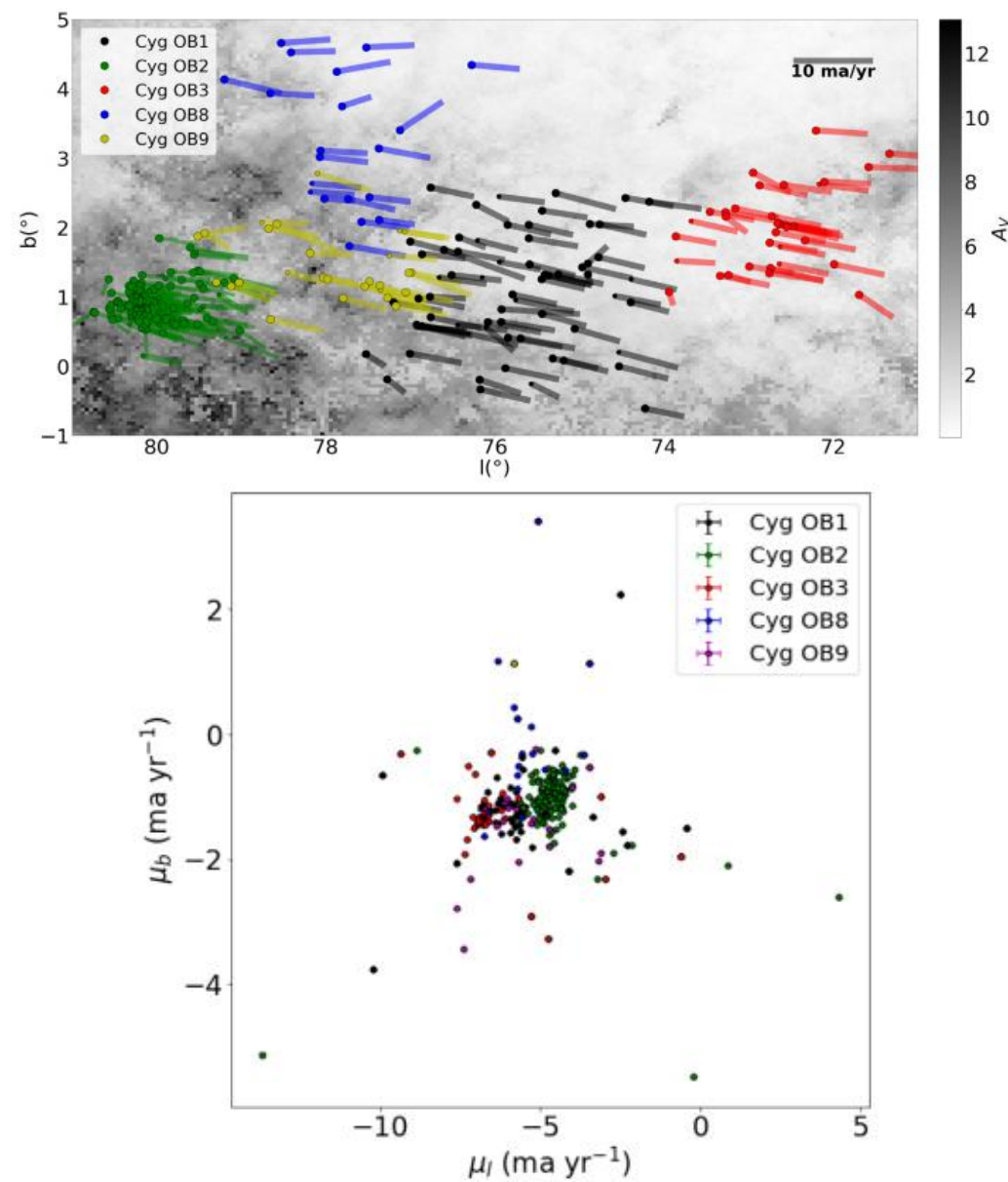
Introduction

- Many OB stars are assembled in associations (McKee & Williams 1997). As a transitional phase between star-forming regions and the field population of stars, OB associations are important to study in order to better understand Galactic evolution (Wright 2020).
- The two main scenarios for the origin of OB associations are the expanding star cluster and hierarchical star formation models. According to the former, OB associations constitute the expanded remnants of dense star clusters (Blaauw 1964), following a disruption of their parent molecular cloud through a feedback phase once massive stars emerge (Hills 1980). According to the latter, stars form in groups with a wide variety of sizes and densities and most are unbound and disperse from birth (Kruijssen 2012). It is therefore considered important to search for expansion patterns in OB associations.
- The goal of this work is to study the kinematics of OB associations to search for evidence of expansion, using reliable and updated membership lists. This requires them to either refine the membership of existing OB associations or identify such systems from scratch. To that aim, they turn their attention to the Cygnus region as a first target since it contains many OB associations and is rich in OB stars (Reipurth & Schneider 2008).



The Existing OB Associations In Cygnus

- Their focus is on a 60 deg² area in the Cygnus constellation spanned by $l = [71^\circ, 81^\circ]$ and $b = [-1^\circ, 5^\circ]$. This region contains the OB associations Cyg OB1, OB2, OB3, OB8, and OB9, the five most well-studied associations in Cygnus. For this work, they use the list of 164 OB stars in Cyg OB1, OB3, OB8, and OB9 from Blaha & Humphreys (1989). For Cyg OB2, they use the updated census of OB stars from Berlanas et al (2019). This gave them a total of 341 OB stars.
- They attempted to refine the association membership, by removing outliers in distance and proper motion, and also used a number of modern clustering algorithms applied to this list of OB stars to ‘re-discover’ these associations, but only Cyg OB2 and OB3 appeared to show any level of kinematic coherence that would suggest they are true associations. The other associations, Cyg OB1, OB8, and OB9, are not genuine OB associations. It would therefore be pertinent to reconsider the possible OB associations in Cygnus, starting from the ground up.



Identifying And Characterizing OB Stars

- They use photometry and astrometry from **IGAPS** (INT Galactic Plane Survey, providing g-, r-, i-band photometry, Drew et al 2005, Monguio et al 2020), **2MASS** (Two-Micron All-Sky Survey, providing J-, H-, and Ks-band photometry, Cutri et al 2003), **UKIDSS** (United Kingdom Infrared Deep Sky Survey, providing deeper J-, H- and K-band photometry, Lucas et al 2008), and **Gaia EDR3** (Gaia Collaboration 2016, 2020; Riello et al 2020), providing G-, GBP- and GRP-band photometry.
- They cross-match Gaia EDR3 with 2MASS, UKIDSS, and IGAPS, and screened data according to conditions:
 - they discarded all unreliable photometry
 - they exclude as well photometry with either $J < 13.25$, $H < 12.75$, and $K < 12$
 - $\text{RUWE} < 1.4$
 - they require at least one good photometric measurement in a blue band (g, BP or G) and one in a near-IR band
- Following all cuts, they were left with a sample of **20 498 objects**, and selected the OB stars they are interested in.
- **Fig. 7** shows the broad spatial and kinematic distribution of their SED-fitted OB stars ($\log(\text{Teff}) > 4$). The spatial distribution (top panel) shows a broad density gradient as a function of Galactic latitude, as expected, **with multiple overdensities that might represent OB associations** (including one in the position of Cyg OB2 at $l \sim 80^\circ$, $b \sim 1^\circ$).

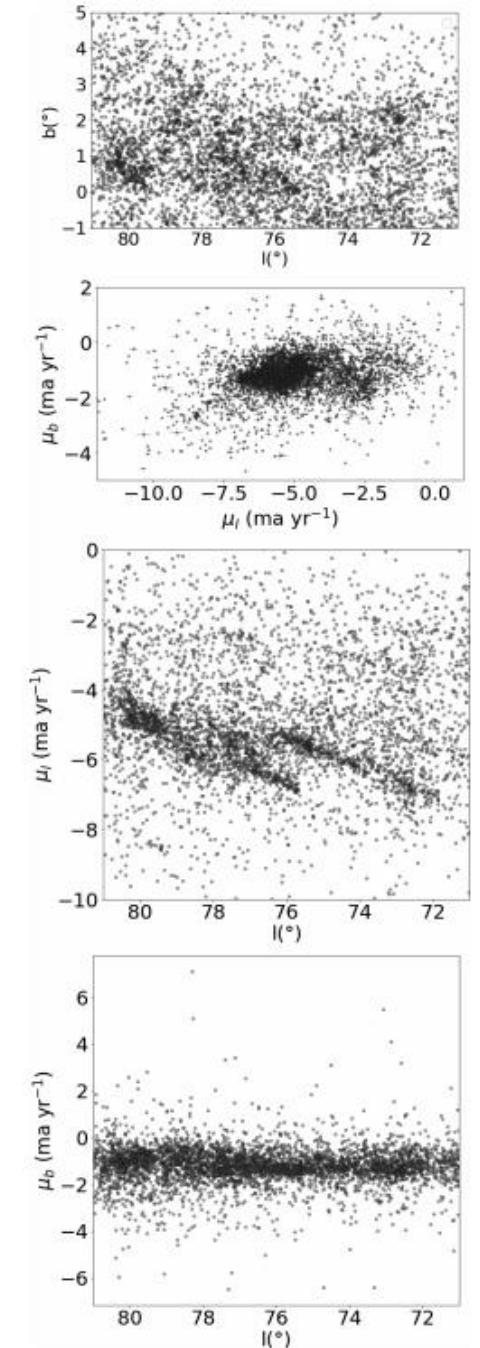


Figure 7. Spatial and proper motion distributions of the 4680 objects fitted with $\log(T_{\text{eff}}) > 4$.

Identifying New OB Associations

- For the purpose of identifying OB associations, they limit our sample of stars to those with $\log(\text{Teff}) > 4.2$ (approximately equivalent to spectral type B5 or earlier), which gives them 1349 stars. This limits them to a sample of more massive and therefore younger stars with which to identify young groups.
- They define a grid with a cell size of 0.1° and at each point in this grid, they select the ten nearest stars from the sample of 1349 stars. They then perform a Kolmogorov–Smirnov (KS) test comparing the proper motion distribution of these ten stars with the proper motion distribution of all 1349 stars. They do this for both the proper motion in l and in b , obtaining a p-value for each, and then multiply them together. The result is the probability that the kinematics of stars in that area are consistent with that of the wider population.

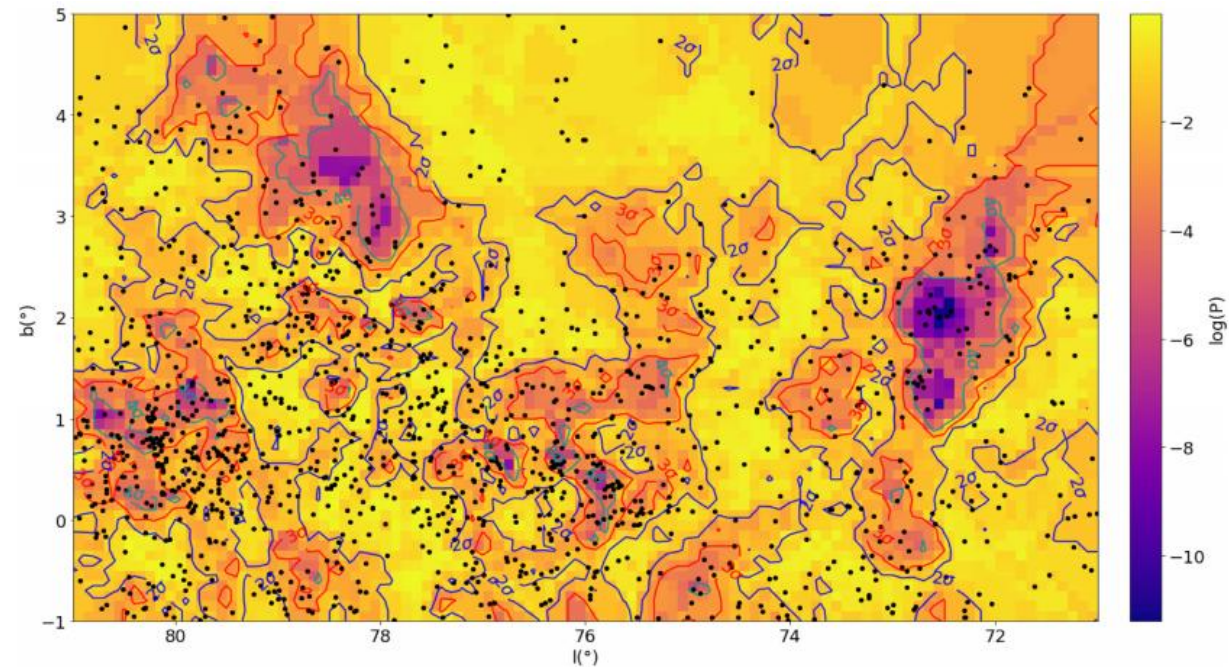


Figure 8. The Cygnus region, colour-coded according to probability, $\log(P)$, that the kinematics of stars in that vicinity are consistent with that of the wider population. The 2σ , 3σ , 4σ contours represent levels at $\log(P) = -1.3$, -2.6 , and -4.2 , respectively.

Identifying New OB Associations

- To identify stars in a given group, they choose the 3σ contour level and define all stars falling within such a contour as being tentatively part of that group. And they required each group to contain a minimum of 10 stars.
- From this, they find the following groups:
 - (i) Group A is located in the upper right-hand part of Fig. 8, with $l = 71.5^\circ\text{--}73^\circ$ and $b = 0.5^\circ\text{--}3.0^\circ$.
 - (ii) Group B spans the upper left-hand part of Fig. 8, in the region $l > 77^\circ\text{--}80^\circ$ and $b = 2.5^\circ\text{--}5.0^\circ$.
 - (iii) They initially defined a third group in the region of l from 75 to 77.5 and b from -0.5 to 2° , but further investigation (see later) suggested this constituted two groups with distinct μ_l distributions and so this was separated into two groups, C and D, with μ_l less than and greater than $\mu_l = -6$ mas yr $^{-1}$.
 - (iv) The group in the lower left-hand part of Fig. 8 corresponds to Cyg OB2 and its surrounding. It forms group E.

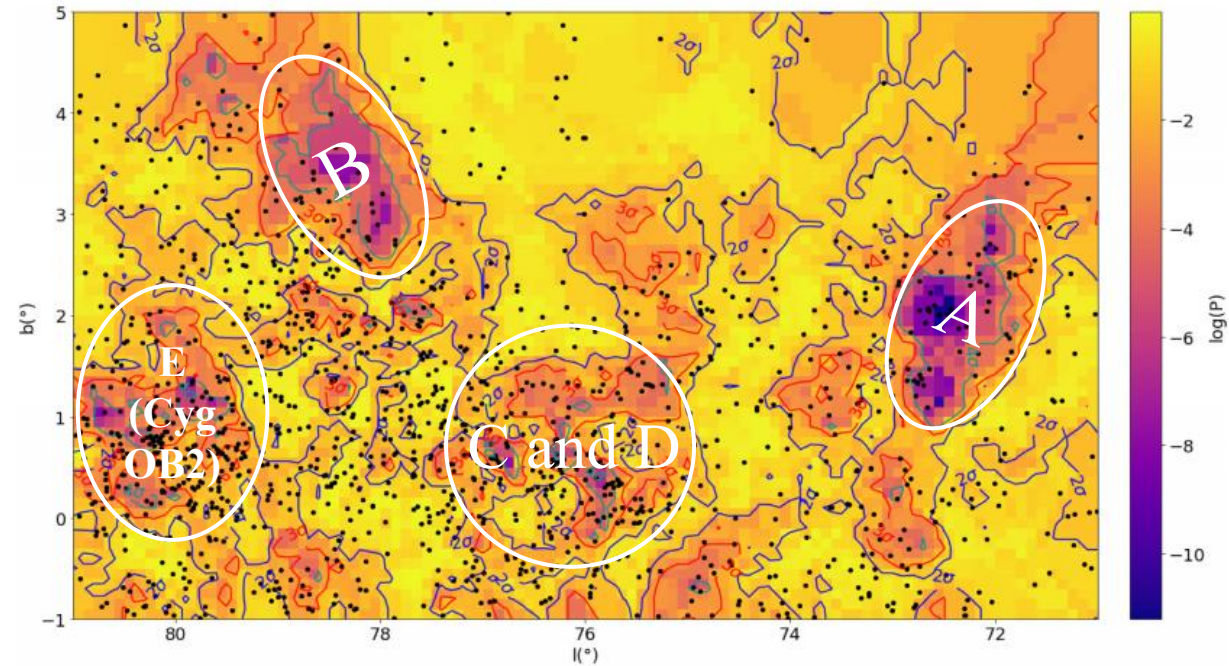


Figure 8. The Cygnus region, colour-coded according to probability, $\log(P)$, that the kinematics of stars in that vicinity are consistent with that of the wider population. The 2σ , 3σ , 4σ contours represent levels at $\log(P) = -1.3$, -2.6 , and -4.2 , respectively.

Identifying New OB Associations

- The membership of the existing groups to a total of 123, 93, 93, 86, and 163 stars.
- In later analysis of the kinematics of these stars, they became aware of a ‘gap’ between groups A and D. They identified the stars that fell between groups A and D in both l . This resulted in a group of 155 stars named Group F.
- They calculated the ages, determining groups B, C, and E as the youngest (due to the presence of very luminous stars within them), and groups A, D, and F as the oldest (due to the presence of stars at or beyond the 10-Myr isochrone).

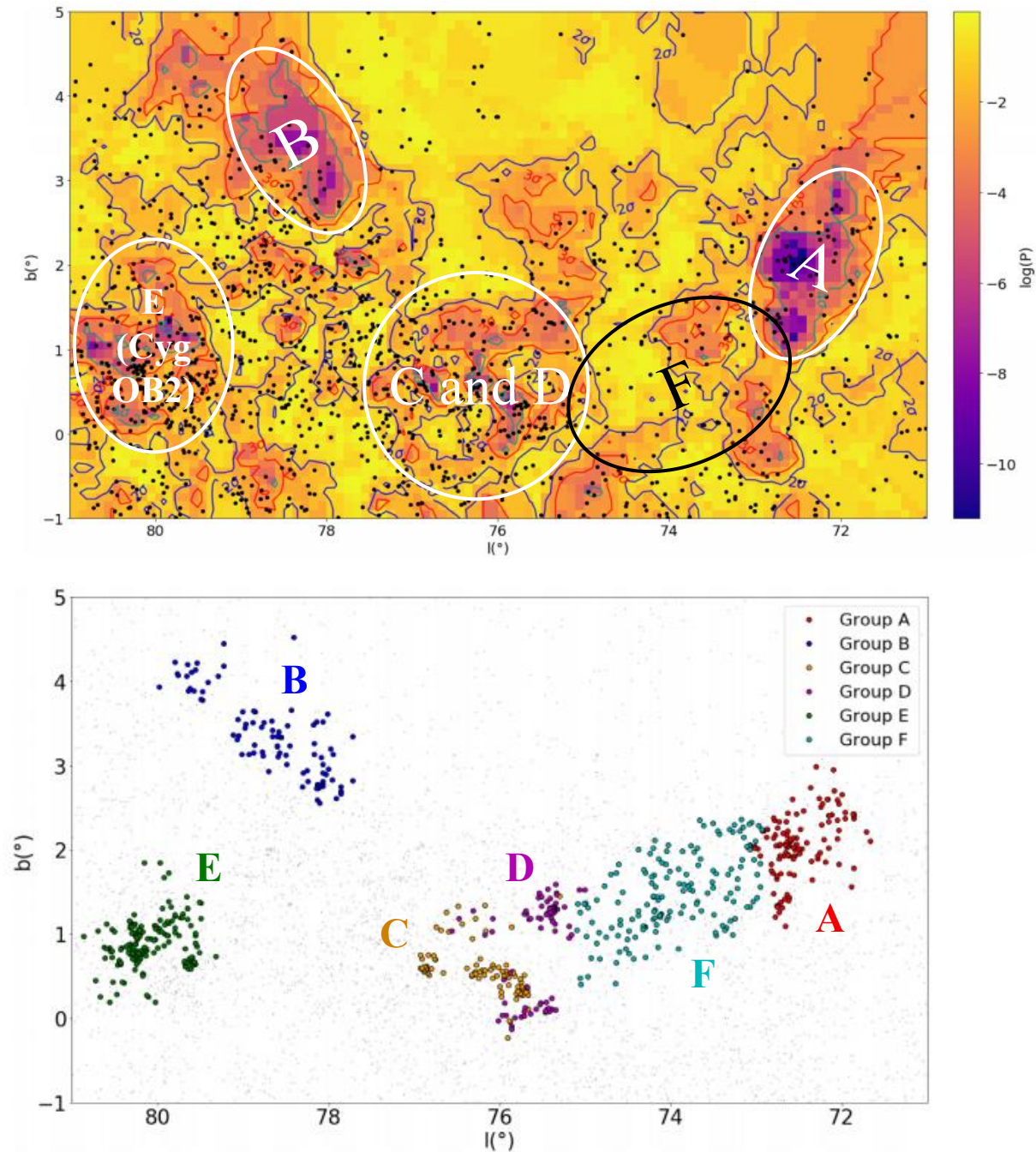


Figure 10. Spatial distribution of all the identified new OB groups (coloured symbols), plotted against the field OB stars (black dots).

Identifying New OB Associatio

- They compared the membership of their groups with that of the historical associations: while Cyg OB2 stands out as a real group (corresponding roughly to our group E) and Cyg OB3 has some overlap with group A, the same is not true for the other groups, which show very little overlap with the historical OB associations (typically 5–20 per cent of the historical association members are found in the nearest new groups we identify).

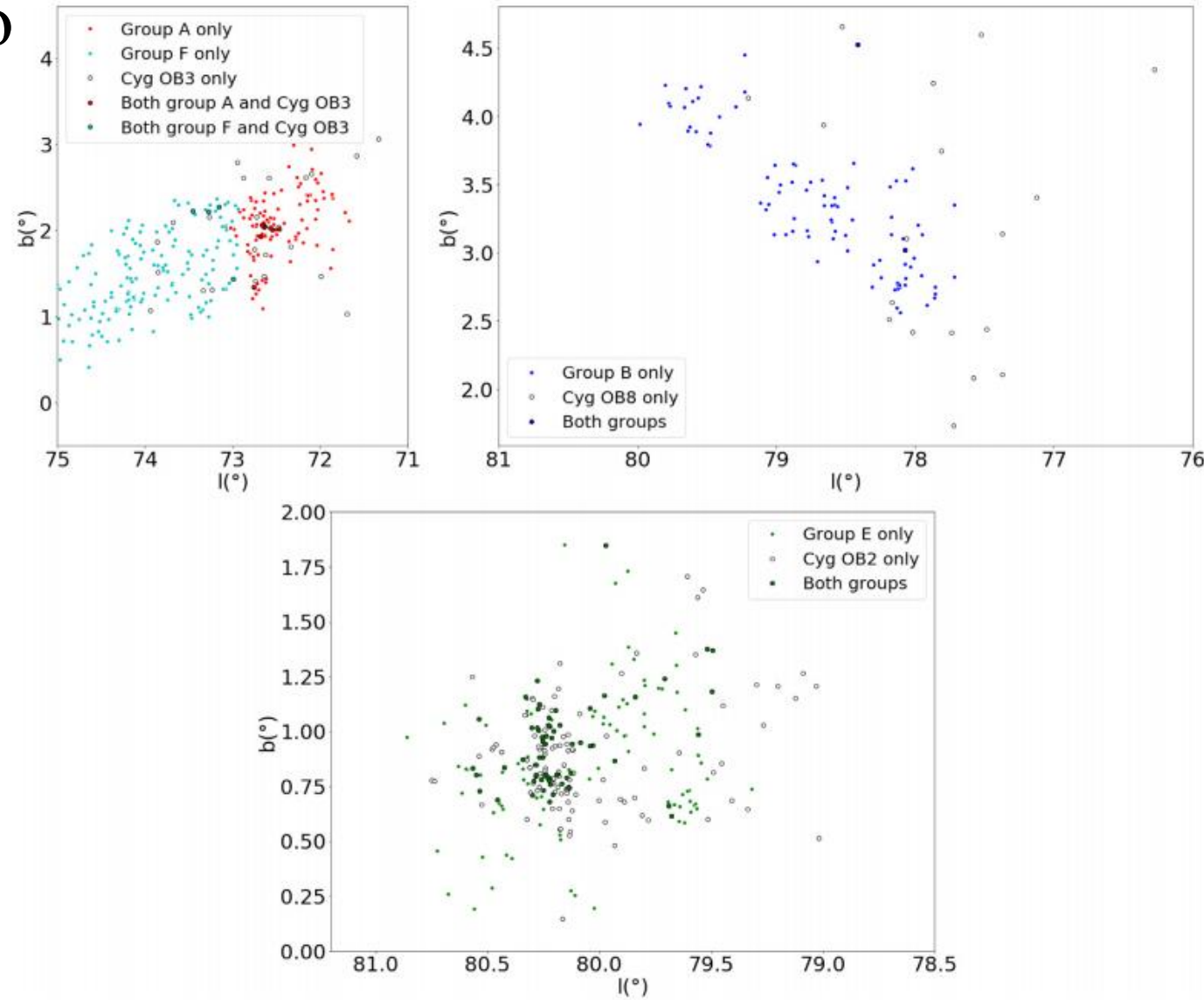


Figure A1. Comparison between our new groups and the historical associations Cyg OB2, OB3, and OB8.

Analysis of the New OB Associations

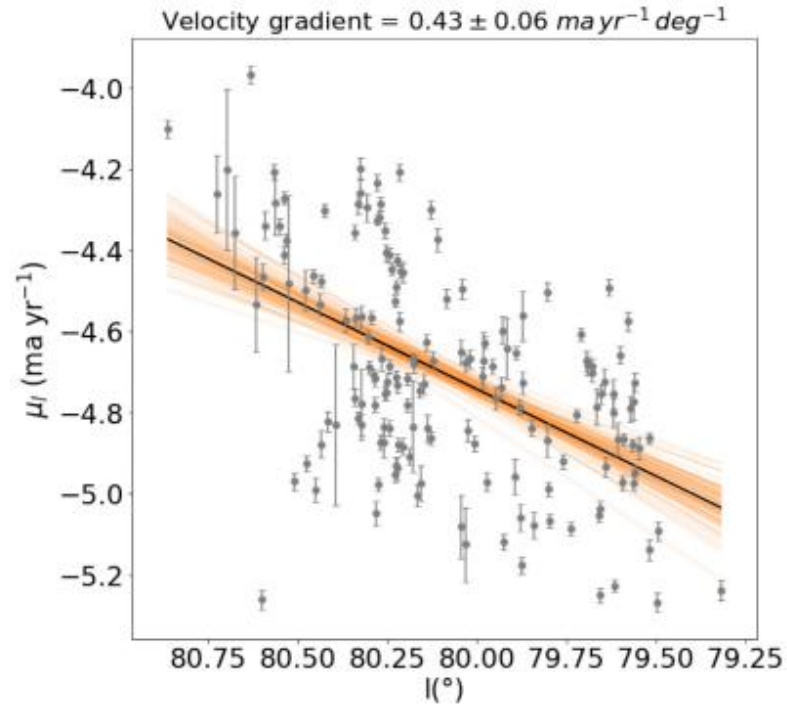


Figure 14. Results of the MCMC fit between position and proper motion for the l direction for group E. In total, 100 random samples have been drawn from the posterior distribution. The black line corresponds to the best-fitting value for the velocity gradient which has been indicated on the top of the plot.

Parameters	Units	Group A	Group B	Group C	Group D	Group E	Group F
$RA(ICRS)_m$	deg	301.45	304.37	305.47	304.34	308.08	302.95
$DE(ICRS)_m$	deg	35.68	41.43	37.87	37.64	41.30	36.58
l_m	deg	72.61	78.58	76.11	75.44	80.19	74.04
b_m	deg	2.06	3.31	0.54	1.19	0.85	1.44
d_m	pc	1894.5	1726.3	1713.1	2000.1	1674.0	1985.2
μ_{l_m}	mas yr ⁻¹	-6.90	-5.47	-6.57	-5.55	-4.72	-6.11
σ_{μ_l}	mas yr ⁻¹	0.24	0.34	0.27	0.16	0.27	0.30
μ_{b_m}	mas yr ⁻¹	-1.35	-0.59	-1.19	-1.34	-0.96	-1.33
σ_{μ_b}	mas yr ⁻¹	0.17	0.27	0.12	0.14	0.25	0.1
σ_{v_l}	km s ⁻¹	$2.20^{+0.55}_{-0.47}$	$2.72^{+0.47}_{-0.37}$	$2.24^{+0.46}_{-0.35}$	$1.53^{+0.45}_{-0.41}$	$2.15^{+0.66}_{-0.45}$	$2.80^{+0.58}_{-0.48}$
σ_{v_b}	km s ⁻¹	$1.55^{+0.32}_{-0.24}$	$2.18^{+0.41}_{-0.33}$	$0.96^{+0.22}_{-0.18}$	$1.32^{+0.30}_{-0.26}$	$1.96^{+0.52}_{-0.29}$	$1.50^{+0.30}_{-0.25}$
Observed number of B stars		112^{+3}_{-3}	82^{+3}_{-2}	76^{+2}_{-3}	75^{+2}_{-3}	110^{+4}_{-3}	139^{+3}_{-3}
Observed number of O stars		3^{+1}_{-1}	4^{+1}_{-1}	10^{+1}_{-2}	4^{+2}_{-1}	35^{+2}_{-3}	5^{+2}_{-1}
Corrected number of O stars		13^{+4}_{-3}	11^{+4}_{-3}	12^{+4}_{-3}	11^{+4}_{-3}	23^{+6}_{-5}	17^{+4}_{-5}
Estimated total stellar mass	M_{\odot}	2344^{+275}_{-252}	1978^{+245}_{-224}	2165^{+245}_{-224}	1569^{+215}_{-192}	4198^{+354}_{-319}	2955^{+349}_{-269}
Velocity gradient (l)	mas yr ⁻¹ deg ⁻¹	0.24 ± 0.07	0.39 ± 0.04	0.38 ± 0.04	0.20 ± 0.05	0.43 ± 0.06	0.35 ± 0.03
Velocity gradient (l)	km s ⁻¹ pc ⁻¹	0.07 ± 0.02	0.11 ± 0.01	0.10 ± 0.01	0.05 ± 0.01	0.12 ± 0.01	0.09 ± 0.01
Velocity gradient (b)	mas yr ⁻¹ deg ⁻¹	0.34 ± 0.04	-0.03 ± 0.04	0.10 ± 0.04	0.07 ± 0.03	0.16 ± 0.05	0.06 ± 0.03
Velocity gradient (b)	km s ⁻¹ pc ⁻¹	0.09 ± 0.01	-0.01 ± 0.01	0.03 ± 0.01	0.02 ± 0.01	0.04 ± 0.01	0.02 ± 0.01
Expansion age (l)	Myr	13.98 ± 3.99	8.89 ± 0.81	7.93 ± 0.80	19.57 ± 3.91	8.37 ± 0.70	10.87 ± 1.21
Expansion age (b)	Myr	10.87 ± 1.21	—	32.62 ± 10.87	—	24.46 ± 6.11	—

- To determine whether the groups are expanding, they search for evidence of velocity gradients in the kinematics of our stars. To compute the velocity gradients, they fit a linear relationship using an MCMC simulation and the emcee package, and obtain velocity gradients for each group. The velocity gradients are generally anisotropic and larger in the l direction compared to the b direction. The expansion ages in the l and b directions do not agree for any of the groups except group A.

Analysis of the New OB Associations

- In the right-hand panel of Fig. 11, the proper motion in Galactic longitude is plotted against Galactic longitude. A very clear trend of increasing proper motion is shown as a function of Galactic longitude for the stars in two combinations of associations: groups A, D, and F at low longitudes and groups B, C, and E at high longitudes. These two sets correspond to the three young groups and the three old groups, hinting at a connection in both dynamics and age. This pattern repeats itself on a scale of five degrees in longitude (from $l = 81^\circ$ – 76° and from $l = 76^\circ$ – 71°). and approximately 3 mas yr^{-1} in proper motion. At a rough distance of 1800 pc, these equate to $\sim 150 \text{ pc}$ and $\sim 25 \text{ km s}^{-1}$. No such pattern is seen for μ_b as a function of either l or b .

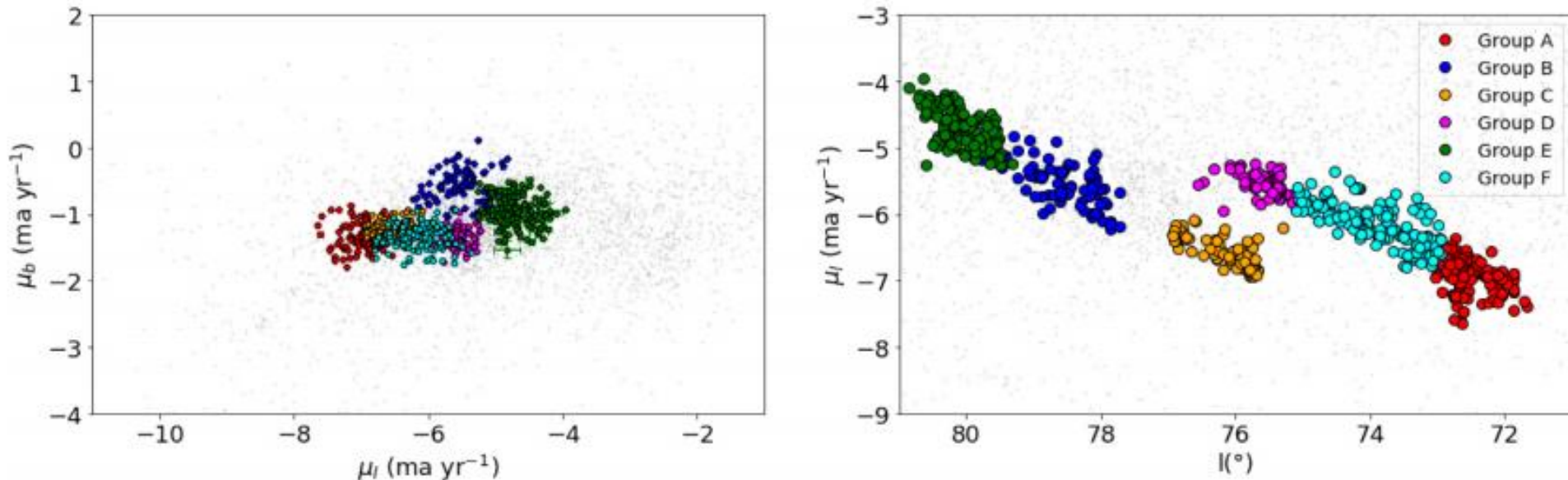


Figure 11. Left-hand panel: proper motion distribution of all six new OB groups (coloured symbols), plotted against the field OB stars (black dots). Right-hand panel: proper motion in l plotted against l for the same objects. The uncertainties in μ_l are comparable to, or smaller than, the symbol size, and thus are not shown.

Discussion and Conclusion

- Our main results are as follows:
 - (i) Most of the historical OB associations in the Cygnus region lack kinematic coherence and therefore do not appear to be genuine OB associations. They identified six new systems that they compared to the previous divisions. There is a strong overlap between their group E and Cyg OB2, a partial overlap between group A and Cyg OB3, but no significant overlap between their other groups and the other historical associations.
 - (ii) They calculated the broad properties of each new association, including estimates of their total stellar mass, quantifying their incompleteness. Group E (Cyg OB2) contains by far the largest number of O-type stars and is the most massive.
 - (iii) They calculated the velocity dispersions of each group and searched for evidence that they are expanding. They found strong evidence of expansion for all of the groups in the l direction and in groups A, C, and E in the b direction.
 - (iv) They discovered a correlation between l and μ_l on large scales across the entire Cygnus region, specifically connecting the three oldest and the three youngest groups, thus showing a connection between age and dynamics.